Volume 2 / Issue 2 / December 2022

Research Article

Cytocompatibility of Novel Algae-PLA Membranes For Guided Bone Regeneration At The Level of Types I, III And V Collagen Expression

Yahya Acil, DDS, PhD[1], Fatih Karayürek, DDS, PhD[2], Hela Helene Uplegger, DDS, PhD[3], Oral Cenk Aktas, DDS, PhD[4], Christian Flörke, DDS, PhD[1], Theresa Kohlhaas, DDS, PhD[1], Merve Olcay Duman, DDS, PhD[1], Selin Sayin, DDS, PhD[5], Emine Şükran Okudan, DDS, PhD[6] Ilker Eyüp Saygili, DDS, PhD[7], Aydin Gülses, DDS, PhD[1*]

[1]*University Hospital of Schleswig-Holstein, Department of Oral and Maxillofacial Surgery,Kiel, Germany*
[2]*Karabük University, Faculty of Dentistry, Department of Periodontics, Karabuk, Turkey*
[3]*RWTH Aachen University, Department of Biomedical Engineering, Aachen, Germany*
[4]*Kiel University, Faculty of Engineering, Institute of Materials Science, Department of Multicomponent Materials, Kiel, Germany*
[5]*Iskenderun Technical University, Marine Science and Technology Faculty, Hatay, Turkey*
[6]*Akdeniz University, Marine Sciences, Antalya, Turkey*
[7]*SANKO University, Department of Medical Biochemistry, SANKO Gaziantep,*
**Corresponding author: aguelses@mkg.uni-kiel.de*

Acil, Yahya., Karayürek, Fatih., Uplegger, H. Helene., Aktas, O. Cenk., Flörke, Christian., Kohlhaas, Theresa., Olcay Duman, Merve., Sayin, Selin., Saygili I. Eyüp. & Gülses, Aydin. "Cytocompatibility of Novel Algae-PLA Membranes For Guided Bone Regeneration At The Level of Types I, III And V Collagen Expression". *Acta Stomatologica Cappadocia.* 2;2 (December 2022): 18-44.
DOI: https://doi.org/10.54995/ASC.2.2.3
Received: 24.11.2022; Accepted: 12.12.2022

Cytocompatibility of Novel Algae-PLA Membranes For Guided Bone Regeneration At The Level of Types I, III And V Collagen Expression

Yahya Acil, Fatih Karayürek, Hela Helene Uplegger, Oral Cenk Aktas, Christian Flörke, Theresa Kohlhaas, Merve Olcay Duman, Selin Sayin, Emine Şükran Okudan, Ilker Eyüp Saygili, Aydin Gülses

Abstract

Statement of the problem: In recent years, the development of innovative and increasingly optimized barrier membranes has focused on marine algae, which as a biopolymer can form a membrane composite together with polylactic acid, thus a combination could show numerous advantages such as antioxidant, antitumor, antibacterial, antiviral as well as antiallergic properties. Furthermore, algae can be produced in an ecologically sustainable way and offer an alternative for patients who refuse treatment with bovine or porcine derived membranes due to ethical or religious reasons.

Objective: In this study, four different algal membranes were evaluated for their cytocompatibility with cultured human fibroblasts and osteoblasts.

Materials & Methods: Mem-Lok® (Collagen Matrix, New Jersey, USA) as a resorbable collagen membrane and ArgonautTM (Botiss Biomaterials, Zossen, Germany) as a native pericardium GBR/GTR membrane served as reference membranes (RMs). As the negative control cells incubated with normal culture medium only were used. In addition to the cell viability and proliferation assays water soluble tetrazolium (WST), MTT and BrdU, a real time semi-quantitative real time PCR (RT-PCR) was developed to investigate in vitro cytocompatibility at the level of types I, III and V collagen expression. A sandblasted-large grid-acid ached titanium surface (Dentcon® Dental Implant Systems, Ankara, Turkey) served as a positive inactive control group for osteoblastic cytocompatibility.

Results: For human osteoblasts, the algal membranes showed very good proliferation levels in WST-1, MTT as well as BrdU, indicating cytocompatibility. Examination of the expression behavior of type I, type III, and type V collagen genes showed no evaluable results. However, the RT-PCR should be repeated with the incorporated optimizations to be able to make a statement regarding the success of bone, skin, and connective tissue regeneration after a possible application of the membrane in maxillofacial injury treatment.

Conclusion: The investigated collagen types are essential for a proper healing of defects in both soft and bone tissue, as they have fundamental functions such as stability and structural integrity of the tissues.

Keywords: Brown Algae, Collagen, Membrane, Red algae, Osteoblasts, Guided Tissue Regeneration, Guided Bissue Regeneration

Introduction

Oral and maxillofacial injuries as bone defects can be considered one of the most devastating injuries in traumatology and oncology, as they can lead to deformities in the face. The face is an always visible, very representative, and an individual feature for us humans. For this reason, the trauma of the face can have strong emotional and psychological consequences. In addition, maxillofacial injuries also have an economic impact on the national health care system (NHS). In the last years, the development of bio-membranes has represented a successful treatment for the correction of bone defects in the facial region.[1] Maxillofacial injuries as bone defects are often treated by mean of bone grafts. This plays a crucial aspect for the type of bone regeneration, which is in this case new bone formation beyond the genetically determined skeletal envelope.[2]

Bone grafts can only form new bone through direct osteogenesis, osteoconduction or osteoinduction. However, for a successful healing process, not only the bone must be regenerated, but also the surrounding tissue, which was either also injured in the original fracture or damaged by the treatment procedure. Therefore, it is crucial that all phases of soft tissue wound healing - hemostasis, inflammation, proliferation, and remodeling - take place.[3]

The guided tissue regeneration (GTR) is a therapeutic approach to prioritize the tissues and cells that have priority in the healing process, aiming for clinical healing that is closest to the original structures of the lost supporting tissues. According to the GTR principle, the new formation or rather regeneration of a certain tissue is ensured when cells of the specific damaged or fully lost tissue can repopulate the site of defect during healing. That also applies to guided bone regeneration (GBR), in which undesired non-osteogenic cells are prevented from proliferating into the defect to allow osteogenic cells to repopulate the osseous wound.[2] In dentistry, barrier membranes are used for GTR and GBR.[4] Membranes are thin layers of material that locally separate areas from one another, while also providing a barrier function for certain substances. The principle behind this is to allow osseous regeneration prior to soft tissue migration into the area of interest. The membrane thus prevents the ingrowth of connective tissue cells, fibroblasts, into the bone defects. This allows the slower-growing bone cells, osteoblasts, to regenerate the bone undisturbed.[5] Membranes provide a support function for the soft tissue surrounding the defect. This is essential so that the blood clot, which is important for bone remodeling, can form in the gap. There are many different types of membranes, with a basic distinction between resorbable and non-resorbable. The non-absorbable membranes are made of synthetic polymers and metals, or composites of these.[5] Although collagen-based membranes

are mostly used in the treatment of bone defects in dentistry, alginate-based products have also been used in recent years.[4] It is derived from seaweed and has a similar structure to the extracellular matrix (ECM) and good biocompatible properties. Sasaki et al. states that in application as a membrane in GBR, alginate showed sufficient results, but not significantly better than its commercial equivalents.[4]

Biodegradable synthetic polymers are aliphatic polyesters, for instance polylactide acid (PLA). PLA is also used as a membrane in dentistry. In addition to its barrier function, it has the advantage that it can be manufactured industrially. By adjusting the composition of the polymer, its mechanical properties and biodegradability can be modified. PLA membranes have a low hydrophobicity and higher degradability compared to other aliphatic polyester membranes, resulting in a lower lifetime. Therefore, these membranes are used in small bone defects and in combination with bone graft substitutes.[4,5] Marine algae (MA) are particularly promising due to their antioxidant, antitumor, antibacterial, antiviral as well as antiallergic properties. By these properties the algae are promising sources for biopolymers in dentistry.[6] In addition, algae are abundant as they are found in various seas near the coast.[7] They are therefore a more economically sustainable and cost-effective alternative to animals as a source of biopolymers.

The aim of current study is to assess the *in vitro* cytocompatibility of novel algae-PLA membranes at the level of types I, III and V collagen expression**.**

Materials & Methods

The study was approved by "Ethik Kommission" (D 640/20) of Medical Faculty of Christian Albrechts University. The cells seeded were obtained from the rest-tissues of individuals who underwent oral surgical interventions at the Department of Oral and Maxillofacial Surgery, Universitätsklinikum Schleswig Holstein, Kiel- Germany.

The study designs

In this study, four different algal membranes were evaluated for their cytocompatibility with cultured human fibroblasts and osteoblasts. Mem-Lok® as a resorbable collagen membrane and Argonaut™ as a native pericardium GBR/GTR membrane served as reference membranes (RMs). As the negative control cells incubated with normal culture medium only were used. In addition to the cell viability and proliferation assays water soluble tetrazolium (WST), MTT and BrdU, a real time semi-quantitative real time PCR (RT-PCR) was developed to investigate *in vitro* cytocompatibility at the level of types I, III and V collagen expression.

Algae membranes

The algal membranes for this work were provided by the Marine Science and Technology Faculty of Iskenderun Technical University in Iskenderun/Hatay, Turkey. The membranes were prepared from four different species of algae (Table 1); Corallina elongate, Galaxaura oblongata, Cystoseria compressa and Stypopodium schimperi, whereby the first two algae species belong to the class of Rhodophytas and the last two to the class of Phaeophyta. The algae used to produce the membranes were collected from two different locations in the Mediterranean Sea. The Rhodophytas were collected near Antalya, whereas the Phaeophyta were collated near Iskenderun.[8]

Table 1. Overview of algal species, their classification and origin.

Membrane type	Species of algae	Class	Origin
A2 	*Corallina elongate*	*Rhodophyta* (red alga)	Near Antalya, Turkey
A3 	*Galaxaura oblongata*		
A4 	*Cystoseria compressa*	*Phaeophyta* (brown alga)	Near Iskenderun, Turkey
A6 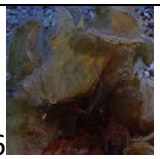	*Stypopodium schimperi*		

The algal membranes consist of a mixture of algal powder (MAP) which was blended with polylactide (PLA) to form a composite. The proportion of MAP in the composite was 5 - 10 %. The production process is schematically shown in Fig. 1 and consists of a first solving step to release the water-soluble substances, followed by several grinding, mixing and sieving steps. After addition of PLA further mixing and grinding was performed to conclude with a pressing and cooling step.[8]

Eluates

To investigate the cytocompatibility of the new algal membranes, both human fibroblasts and human osteoblasts were treated with eluates of these membranes. To prepare the eluates, samples of the different types of membranes were incubated in the normal culture medium of the cells, allowing the soluble substances to leach out. Prior to this, the membranes were each sterilized for 30 min in UV light.

The eluates for performing the proliferation assays were prepared as follows. One sterilized sample of one algal type, 10 mm x 10 mm in size, was placed in 3 ml of culture medium corresponding to the cell type examined and stored in a refrigerator at 7 °C for 24 h. The preparation of eluates for performing the RT-PCR was done in analogous manner. For this purpose, three sterilized algae samples of one membrane type were incubated for 24 h at 7 °C in 10 ml of nutrient medium corresponding to the cell type. Two reference membranes were tested for cytocompatibility in addition to the algal membranes. Therefore, eluates from the membranes Mem Lok® and ArgonautTM were as well prepared as described.

Table 2. Overview of eluate preparation for the two application fields with number of each eluate and corresponding membrane type.

Eluate	Membrane type	WST-1, MTT and BrdU assay	RT-PCR
E1	Mem-Lok®	1x 10 mm x 10 mm in 3 ml nutrient medium corresponding to cell type	3x 10 mm x 10 mm in 10 ml nutrient medium corresponding to cell type
E2	Argonaut™		
E3	A2		
E4	A3		
E5	A4		
E6	A6		

Cell culture

Cells in culture were incubated in a humidified atmosphere at a constant temperature of 37 °C as well as in a constant CO2 level of 5 %. To reduce any kind of possible contamination the cell culture work was performed under a clean bench. The workbench itself and all objects placed under the workbench were disinfected with 70 % ethanol before use. Before the first step of cell culture work, the culture medium and phosphate buffered saline (PBS) were preheated to 37 °C in a water bath.

The adherent human fibroblasts and human osteoblasts were cultured on polystyrene T75 cell culture flasks. Both cell types were cultured in 10 ml of cell-specific media. To supply

sufficient nutrients and dispose dead cells as well as waste, the medium was changed two times per week.

For passaging, the cells were first washed with PBS. After the PBS was discarded, the cells were detached by using an appropriate trypsin solution. For fibroblasts and osteoblasts, 3 ml of 0,5 % EDTA-Trypsin solution diluted ten times in PBS was sufficient. The culture flasks were incubated with the trypsin solution for 3 min. Through this step the adherent cells detached from the cell culture flask plastic. To stop the reaction 7 ml of culture medium were added. The cell suspension was transferred into a 50 ml centrifuge tube and then centrifuged at 200 g. After discarding the supernatant, the cell sediment was resuspended in associated culture medium and seeded into the T75 culture flasks. In each T75 cell culture flask were seeded 50 x 104 cells.

Cell viability and proliferation assays

Cells were counted by Neubauer counting chamber. Following the counting, cells were seeded onto the 96 cavity microtiter plates as schematically seen in Figure 2.

Two standard dilution series of cells were pipetted into the first two columns of the 96-microtiter plate. The dilution steps are shown in Figure 1. The 100 % standard corresponds to a cell number of 5 x 103 in 100 µl culture medium. In the third column, 5 x 103 cells were seeded in each of the eight cavities, which served as a control for the measurement. In columns four to nine, 5 x 103 cells were also seeded in 100 µl of culture medium per cavity. The plate was then incubated for 24 h at 37 °C and 5 % CO2. After incubation, the old medium in columns four to nine was discarded and cells treated with 100 µl of the corresponding eluates for another 24 h in the incubator. One plate per cell type was used for the WST-1, MTT and BrdU assays.

Inactive positive control

A sandblasted-large grid-acid ached titanium surface (Dentcon® Dental Implant Systems, Ankara, Turkey) served as a positive inactive control group for osteoblastic cytocompatibility. The results were not included in the quantitative assessment. Semi-quantification was conducted by SEM.

Figure 1. Illustration of the pipetting scheme for the preparation of microtiter plates for the WST-1, MTT and BrdU assays.

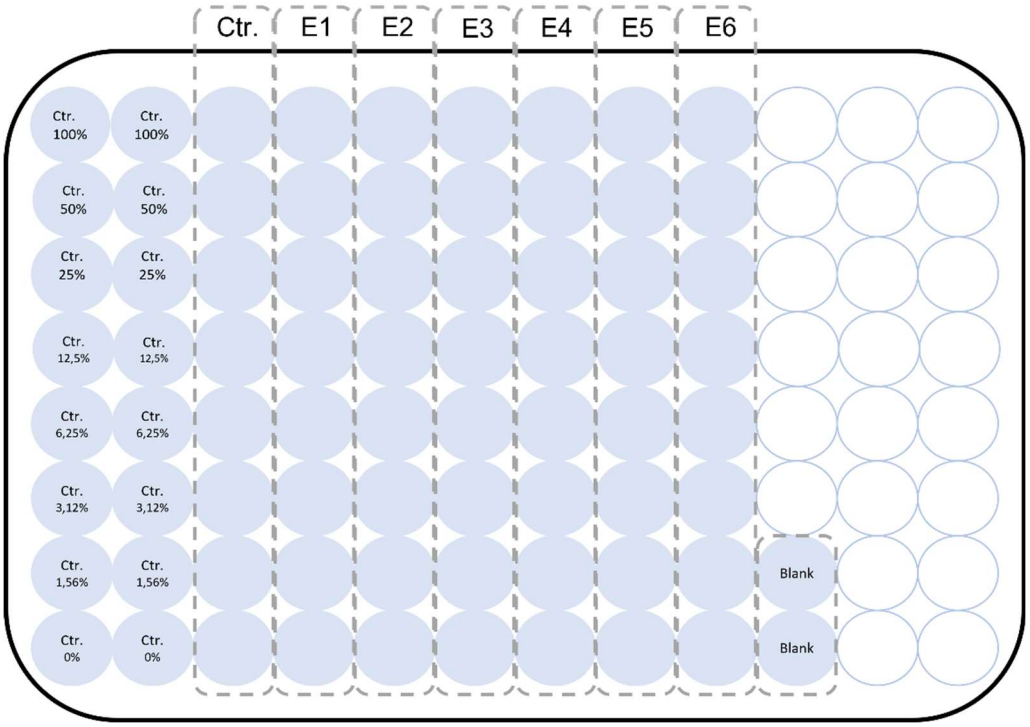

WST Assay

The WST-1 assay is a basic colorimetric cell proliferation assay. The WST-1 reagent is used to detect an intact respiratory chain in the cells examined. In the case of an intact mitochondrial succinate-tetrazolium dehydrogenase, an enzymatic conversion takes place. In this redox reaction, the slightly red tetrazolium salt WST-1 is reduced to dark red-colored, soluble formazan. The reduction was performed by mitochondrial dehydrogenases using NADH/NADPH as co-substrate. The color change is determined photometrically. whereby the intensity is directly proportional to the amount of active mitochondrial dehydrogenase present in the examined cell culture. The more viable cells, the more dehydrogenases are active to reduce the WST-1 reagent. The assay thus serves to determine the metabolic activity of the cells.[9]

The medium was changed and 10 µl of WST-1 reagent added. After four hours of storing the plates in the incubator, they were read in the photometer at 460 nm. The instructions of the Cell-Proliferation Reagent WST-1 Kit were followed.

MTT Assay

The MTT assay is an indicator of cell proliferation and cytotoxicity. The MTT reagent is as well a tetrazolium salt. Detection is based on the reduction of the yellow-colored, water-soluble MTT to violet, water-insoluble formazan (Figure 2).

Figure 2. Redox reaction of the yellow tetrazolium salt MTT to violet formazan.

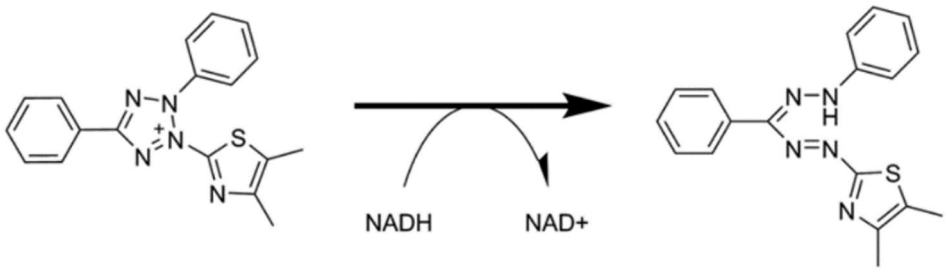

Reduction was done by reducing agent NADH and mitochondrial succinate-dehydrogenase.[9] The quantity of formed formazan is measured photometrically. Any damage to the target cells by cytotoxic substances thereby reduces the cleavage of MTT to formazan. Thus, an objective statement on the cytotoxicity of the treatment can be made.[10]

After the treatment and incubation for 24 h with the eluates, 10 µl of MTT reagent, without prior medium change, was pipetted into each cavity and the cells were placed in the incubator for an additional 4 hours. At the end of this time, 100 µl of solubilization solution was added to them. The plates were kept in the incubator overnight and evaluated in the spectrophotometer at 550 nm the next morning. The instructions of the MTT Cell Proliferation Kit I of Roche were followed.

BrdU assay

The BrdU assay is used to detect DNA replication from growing cells and is thus considered as a proliferation assay. The examined cells are cultured with a labeling medium containing 5-bromo-2'-desoxyuridine (BrdU). BrdU is a pyrimidine analog, that is synthesized from deoxyribose and the nucleobase 5-bromuracil. Cells can take up BrdU and incorporate it into newly synthesized DNA instead of deoxythymidine triphosphate (dTTP). In DNA, it serves as a marker for the replication process. Detection is then performed using a monoclonal anti-BrdU antibody. In the following, an enzyme- or fluorochrome-conjugated secondary antibody recognizes the bound detection antibody. The staining obtained correlates with the number of cells possessing BrdU in their DNA, thereby providing visual evidence of cell division.[11]

The BrdU Cell Proliferation ELISA Kit of Roche was used, and its instructions were followed. After treatment a medium change took place and 10 µl BrdU labeling reagent were pipetted in each cavity. After 24 h incubation, the cells were fixed with 200 µl Fix Denat per cavity for 30 minutes at room temperature (RT). The antibody solution was then applied to the

cells. After two more hours of incubation at RT, the antibody was removed. After three washing steps, 100 µl of substrate solution was pipetted into each cavity for color development. The plates were stored in the dark at RT until the expected color development. The color development reaction was stopped with 50 µl of 1 molar sulfuric acid (H_2SO_4). Eventually, the plates were measured at 450 nm in the spectrophotometer.

Development of a real-time PCR for examination of in-vitro cytocompatibility

For the in vitro investigation of cytocompatibility at the level of types I, III and V collagen expression, human fibroblasts and human osteoblasts were treated with the eluates of the different membrane types. The RNA of the cells was then isolated and subsequently transcribed into cDNA in a one-step RT-PCR. Further, the genes were amplified and semi-quantified.

Cell culture

Human fibroblasts and human osteoblasts were cultured to the fourth passage for experiments. They were then trypsinized and 1x106 cells each transferred to eight 50 ml centrifuge tubes. After one centrifugation step at 200 g, the supernatant was discarded. For the first six 50 ml centrifuge tubes, 10 ml of one of the eluates E1 to E6 (Table 2) were added and the cell sediment resuspended therein. In the other two centrifuge tubes normal culture medium was used to resuspend the cells. They were later used as the control without eluate treatment. The cell suspensions were then placed in a T75 cell culture flask and stored in an incubator for an additional 24 h.

RNA isolation

RNA isolation was performed using the Roche High Pure RNA Isolation Kit and following its instructions. The kit is based on the column method. Here, the cells are lysed using a lysis buffer, the free RNA is precipitated with ethanol and can then bind to the silicate membrane in the column. During isolation, degradation of the RNA is suppressed by inactivated Rnases. DNA, which can also be released during cell lysis, is destroyed by the addition of rDNase. The RNA is eluted from the membrane by three washing steps. Further, washing removes salts and other metabolites so that the eluted RNA can reach the highest possible purity.

RNA quantification

The purity level of RNA probes was determined using the A260/A280 and A260/A230 ratios.[12] For this purpose, 3 µl of each eluted RNA sample was diluted 1:1 with nuclease-free water. The absorbance of the samples was measured using a µDrop plate in the photometer at

the wavelengths 230 nm, 260 nm as well as 280 nm. The evaluation was done with the help of a clinic internal protocol. Based on this photometric determination, the A260/A280 and A260/A230 ratios could be calculated, and the amount of eluted RNA could be determined from the concentration of the sample using Lambert-Beer's law.

Design of specific starter oligonucleotides (primers)

Primers for the COL1A1, COL3A1, and COL5A1 genes were designed using previously opened primer sequences from papers. Table 3 shows the respective sources. The GAPDH primer for the reference gene was purchased from Roche Diagnostics GmbH. All primers used were verified at NCBI primer blast with respect to their CG content, amplicon length, and difference in their melting temperatures, among others. After checking for correctness, the primer sequences were ordered from Eurofins Scientific.

Table 3. Used primers with their sources.

Primer	Source
COL1A1	Perrotti et al[12]
COL3A1	
COL5A1	Wang et al[13]
GAPDH	
GAPDH	Roche Diagnostics GmbH
β-Actin	Liu et al[14]

Semi-quantitative RT-PCR

For the quantification of mRNA expression semi-quantitative RT-PCR was applied using SYBR Green. This method measures after each cycle the amount of target DNA based on the fluorescent marker SYBR Green which intercalates with the double strand DNA (dsDNA) and fluorescent when exited with UV light. The amount of DNA doubles with each cycle thus more SYBR Green molecules react with the dsDNA and the fluorescence intensity increases. When a certain threshold is reached, the fluorescence signal is detected. The cycle threshold (Ct value) is a theoretical value giving the number of cycles after which the amount of target DNA exceeds a theoretical threshold value and is amplified exponentially.[15,16] The Ct value depends on the amount of starting material and is therefore the origin of quantification.[16,17]

In this work the PCR was conducted with the LightCycler 96 applying the EvoScript RNA SYBR Green I Master. The RNA samples of the treated fibroblasts and osteoblasts were analyzed using the following primers: COL1A1, COL3A1 and COL5A1. The RT-PCR Kit is for one step reactions, thus, in the first step of the protocol the RNA samples were reverse

transcribed at 60 °C for 15 min. Following an initial denaturation at 95 °C for 10 min, the amplification consisted of 40 PCR cycles. After a denaturation at 95 °C for ten seconds, an annealing step at 55 °C for 30 sec followed. The elongation proceeded for 45 sec at the optimal temperature of 72 °C for Taq polymerase. Finally, melting was performed for subsequent melt curve analysis.

The primer concentration of 0,4 µM and the amount of 500 ng of RNA template are based on the EvoScript RNA SYBR Green I Master instructions. For each sample three technical replicates were drawn to adjust for technical errors. Expression levels were calculated with the ΔΔCt-method, using GAPDH as housekeeping gene.

Optimization of annealing temperature for RT-PCR

The optimal annealing temperature of the ordered primers was determined using a temperature gradient RT-PCR (Tgrad RT-PCR). According to the instructions of the EvoScript RNA SYBR Green I Master Kit one master mix for each primer was mixed with a primer concentration of 0,4 µM. Then, for each examined primer, one row of the 96-microtiter plate was filled with 20 µl total reaction volume. As samples 500 ng of isolated RNA from untreated human osteogenic sarcoma cells were used. Only for the primer COL3A1, an RNA sample from human fibroblasts was used. The temperature profile corresponded to that of semi-quantitative RT-PCR, with a temperature gradient applied across the columns of the 96-microtiter plate from 50 °C to 65 °C in the annealing step. For the second, repeated Tgrad RT-PCR the interval was adjusted to 55 °C to 65 °C.

Statistical evaluation

Since cells from only one patient were used for both proliferation assays and cells from only two patients were used for RT-PCR, no conclusions about significances can be made. For the evaluations, the respective mean values were calculated, and the error calculation was performed as error propagation based on the standard deviations.

Results

Cell viability and proliferation assays

WST

The WST-1 assay is a cell proliferation assay. The measured optical densities at 460 nm of the samples are plotted relative the control for each of the six membrane types studied. The results of both human osteoblasts and human fibroblasts are shown.

The osteoblasts that had been treated 24 h with the eluates of type A2, A3, A4 and A6 algal membranes exhibited increased proliferation levels in the WST assay compared to the control (Fig 4). Type A2 showed a 20 %, type A3 a 42 % and type A4 a 48 % increased growth to the control. The algal membrane type A6 indicated the highest value with a 50 % increase. In comparison, the RMs Mem-Lok® and Argonaut™ exhibited 30 % lower values than the control. It was noticeable that the error of the optical density ratios for both Mem Lok® membrane with ± 0,167 and Argonaut™ membrane with ± 0,201 was two to four times larger than the error for the algal membranes type A2-A6.

The examination of human fibroblasts after treatment for 24 h showed values above or equal to the control in all groups. In particular, the RMs exhibited enhanced proliferation levels of up to 20 % compared to the control in the case of the Mem-Lok® membrane (Figure 4). As well the investigation of the Argonaut™ membrane showed a clear increase in proliferation of 15 %. In contrast, the algal membranes type A2, type A3 and type A4 indicated no change in proliferation behavior compared to the control. Only membrane type A6 showed a minimal increase of 7 %. Differences in OD ratio errors were also seen in examination of fibroblasts. The error behavior here was contrary to the osteoblasts. The measurement series of the RMs displayed only small errors, whereas the measurements of the algal membranes were three to six times as large with ± 0,268 for type A2 and ± 0,327 for type A3.

Figure 3. Cell proliferation of human osteoblast and fibroblast in WST assay.

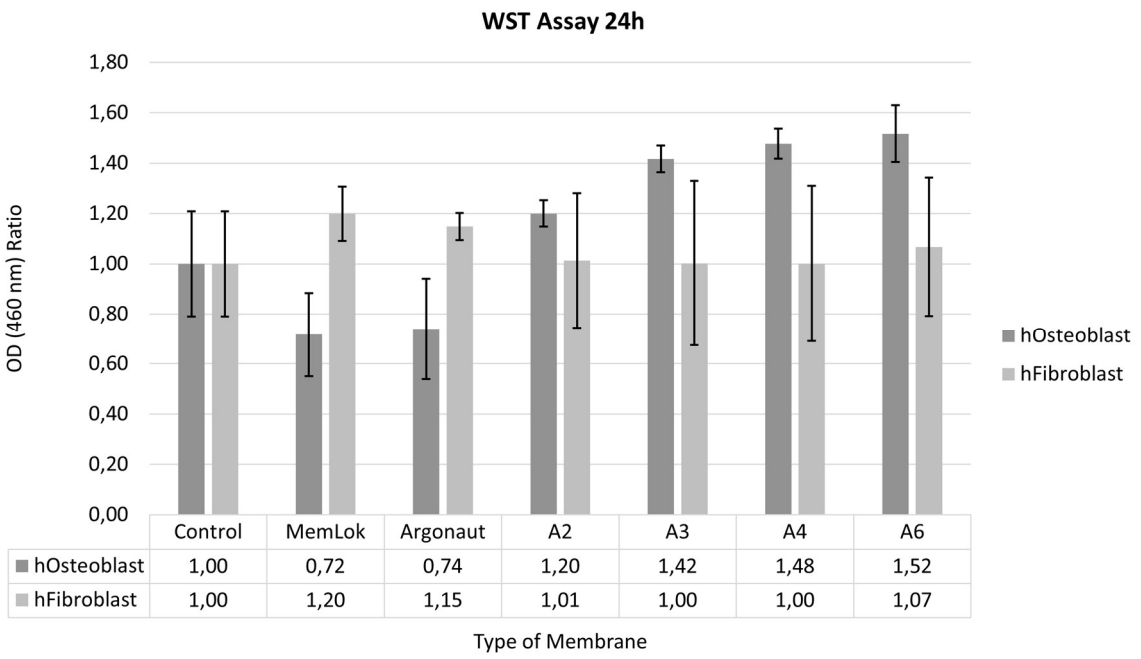

	Control	MemLok	Argonaut	A2	A3	A4	A6
hOsteoblast	1,00	0,72	0,74	1,20	1,42	1,48	1,52
hFibroblast	1,00	1,20	1,15	1,01	1,00	1,00	1,07

The ratio of optical density of both cell types after 24 h treatment with eluates of the four algal membranes A2-A6 and RMs (Mem-Lok® and Argonaut™) is displayed. As control untreated cells were used. The data table shows the optical density ratios calculated from the mean values of the optical density measured as replicates.

MTT Assay

The MTT assay is an indicator of cell proliferation and cytotoxicity. The measured optical densities at 550 nm of the samples are plotted in relation to the optical density of the control in the diagram for each of the six membrane types studied. The results of both human osteoblasts and human fibroblasts are shown.

The MTT test (Figure 5) revealed a similar behavior of osteoblasts and fibroblasts as in the WST test seen in Figure 3. The RMs showed lower proliferation than the control with 86 % for the Mem-Lok® membrane and 89 % for the Argonaut™ membrane. In contrast, the proliferation for algal membranes A2 to A6 was improved by approximately 19 % for each. Thus, it can be said that membrane types A2 to A6 show no cytotoxic effect on osteoblasts in this measurement. However, there may be a cytotoxic effect of the two RMs, as cell proliferation was lower here than in the control group. The errors of the OD ratios in the osteoblast series of measurements were relatively small.

Like the osteoblasts, the fibroblasts exhibited a similar behavior as in the WST assay. Proliferation levels of the RMs were both increased by 50 % compared to the control (Figure

5). In comparison, a decrease in density of fibroblasts was observed after 24 hours of treatment with algal membranes type A2 to A6. There was a 15 % reduction in type A2, 5 % in type A3, and 9 % in type A4. Only the fibroblasts treated with algal membrane A6 achieved the same cell density as the control, namely the untreated fibroblasts. Very contrary to the low proliferation capacity of osteoblasts, fibroblasts measurements revealed that RMs showed no adverse effect on proliferation. However, a cytotoxic effect could not be excluded for the algal membranes A2 to A6 since a reduced OD was found here compared to the control (Figure 4). All groups of fibroblasts measurement series exhibited relatively large errors of OD ratios.

Figure 4. Cell proliferation of human osteoblasts and fibroblasts in MTT assay.

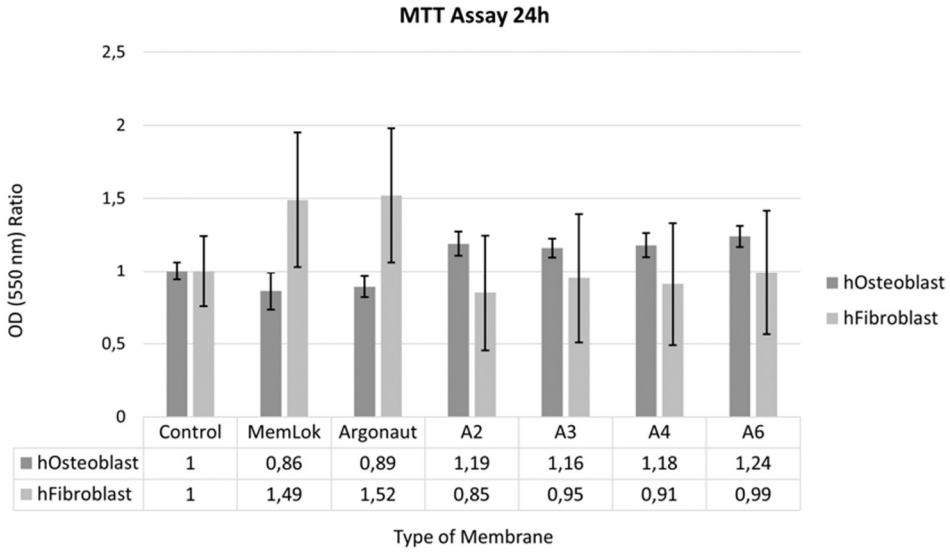

	Control	MemLok	Argonaut	A2	A3	A4	A6
hOsteoblast	1	0,86	0,89	1,19	1,16	1,18	1,24
hFibroblast	1	1,49	1,52	0,85	0,95	0,91	0,99

The ratio of optical density of both cell types after 24h treatment with eluates of the four algal membranes A2-A6 and RMs (Mem-Lok® and Argonaut™) is displayed. As control untreated cells were used. The data table shows the optical density ratios calculated from the mean values of the optical density measured as a replicate.

BrdU Assay

The BrdU immunoassay is as well as the WST and MTT assays considered as a proliferation indicator. The measured optical densities at 450 nm of the samples are plotted in relation to the optical density of the control in the diagram for each of the six membrane types studied. The results of both human osteoblasts and human fibroblasts are shown.

In the BrdU test, both osteoblasts and fibroblasts showed higher or equal proliferation levels as the control in all groups (Figure 5). For the RMs, the osteoblasts reached the same cell density as the control. Type A2 as well as type A4 of the algal membranes promoted the proliferation of the osteoblasts by up to 20 % (Figure 5). After treatment with the algal membranes type A3 and type A6 the cells also exhibited an increased cell density of 18 % and 15 %, respectively, compared to the control. The errors in the OD ratios of the osteoblast's measurement series were relatively small.

As shown in Figure 5, fibroblasts also showed improved proliferation levels in all groups. RM Mem-Lok exhibited the highest proliferation level with 9.9 % increase as well as by algal membrane A4 with 13.6 % increase. Only after treatment with the eluate of algal membrane type A6 the samples achieved only 93 % optical density, which was below the control. The errors in the OD ratios of the fibroblast's measurement series were in the range ± 0,0487 (type A6) to ± 0,162 (Argonaut^{TM}) and were thus slightly larger than the errors of the osteoblast's measurement series.

Figure 5. Cell proliferation of human osteoblasts and fibroblasts in BrdU assay.

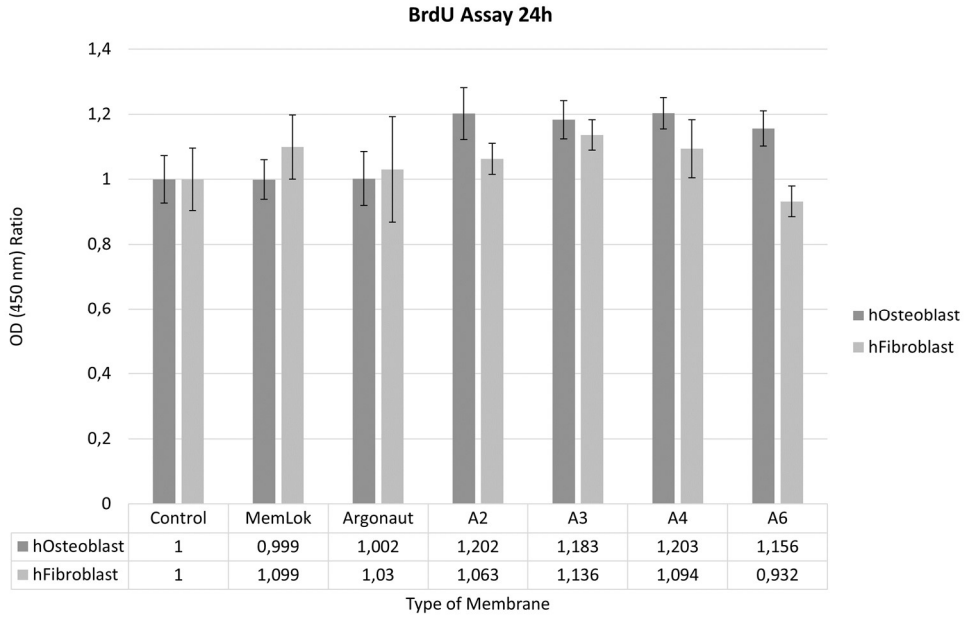

	Control	MemLok	Argonaut	A2	A3	A4	A6
hOsteoblast	1	0,999	1,002	1,202	1,183	1,203	1,156
hFibroblast	1	1,099	1,03	1,063	1,136	1,094	0,932

The ratio of optical density of both cell types after 24h treatment with eluates of the four algal membranes A2-A6 and RMs (Mem-Lok® and ArgonautTM) is displayed. As control untreated cells were used. The data table shows the optical density ratios calculated from the mean values of the optical density measured as a replicate.

RNA Quantification

The purity of the samples, indicated by the A260/A280 ratio, was within the desired range of 2,0 to 2,2 for all samples. Thus, contamination by residual phenol, guanidine, or other reagents used in the extraction protocol can be excluded. In addition, A260/A230 ratios were also determined. Again, all samples had A260/A230 ratios of about 2 or slightly more as for pure RNA. Thus, all isolated RNA samples could be used for the following RT-PCR.

Semi-quantitative RT-PCR

Temperature gradient RT-PCR (Tgrad RT-PCR) is used to determine the optimal annealing or binding temperature for primers. The smaller the Ct value of a measurement, the better the binding behavior and thus the annealing behavior of a primer to its target template. Figure 7 shows the Ct values as a function of temperature profile for the primers COL1A1, COL3A1, COL5A1, GAPDH, and β Actin from the publications. In the first Tgrad RT-PCR, an increasing CT value with increasing temperature was particularly evident for the three collagen primers COL1A1, COL3A1, and COL5A1. In the temperature range from 50,0 °C to 58,0 °C, the Ct values of all three primers ranged from 12 to 17, after which there was a slight increase to a value of 22 for COL1A1 and 26 for COL5A1 at a final temperature of 65,0 °C. The Ct value of primer COL3A1 increased significantly to 36 at a temperature of 65,0 °C. Compared with the collagen primers, the primers of the reference genes GAPDH and β Actin did not show evaluable results (Figure 6). Therefore, Tgrad RT-PCR was repeated for these primers (Figure 6). The Roche GAPDH primer was also included in the analysis. In addition, the temperature gradient was set to 55,0 °C to 65,0 °C.

Figure 6. Results of the second Tgrad RT-PCR.

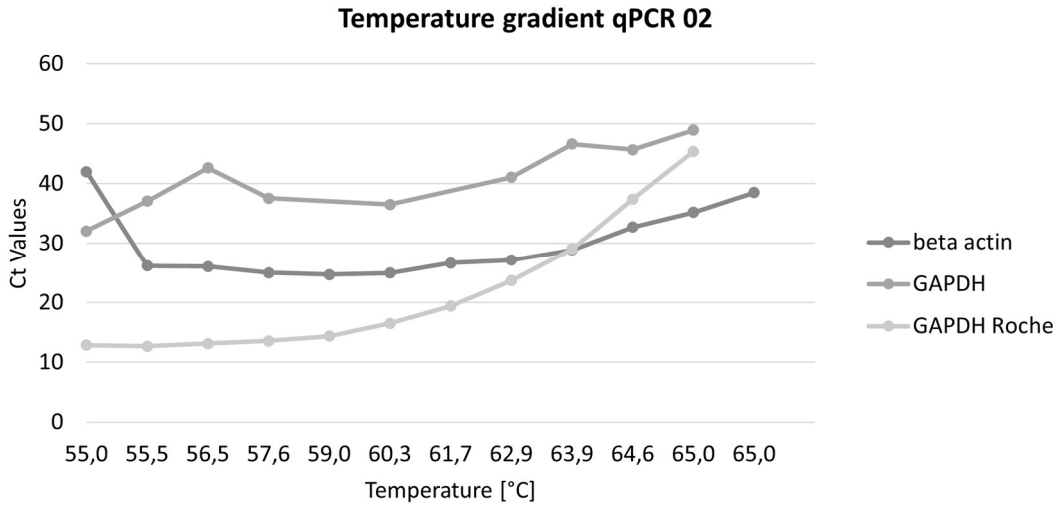

The Ct values of the measurement of the reference genes primers β Actin and two variants of GAPDH are shown as a function of the temperature gradient.

The decision which temperature is optimal for the annealing step in RT-PCR was based on the lowest possible Ct value of all primers at that temperature. When comparing the results from the first and second RT-PCR, it was clear that at 55 °C all collagen primers had the lowest Ct values in the range of 13 to 17 (Figure 7). In the second RT-PCR, Roche's GAPDH primer showed the lowest Ct value of 12 at a temperature of 55 °C. Therefore, Roche GAPDH was selected as the primer for the reference gene in the following studies.

As cytocompatibility of algae membranes has been examined by cell proliferation and viability assays, it should also be investigated by a molecular biology method such as RT-PCR. The examination was performed at the level of type I, III and V collagen expression. Since the RT-PCR has only recently been established for this specific research question, the following experiments are seen as preliminary tests and will be discussed controversially.

The last step of each RT-PCR was a melting step to be able to differentiate in the followed analysis unspecific primer dimers from the amplification products. In fig 9 the melting curves for the RT-PCR with the first fibroblast donor are shown. Negative controls of RNA isolation and negative controls of RT-PCR for primers COL1A1 and COL3A1 revealed primer dimers in the temperature range 71 °C to 77 °C (Figure 7). The melting curves of the replicates for the primer COL1A1 had their maximum at 85,5°C. The peaks of the melting curves of the amplicons for primers COL3A1 and GAPDH overlapped at 80 °C. They exhibited the highest maxima.

Figure 7. Melting curves for the RT-PCR of fibroblast samples of the first doner.

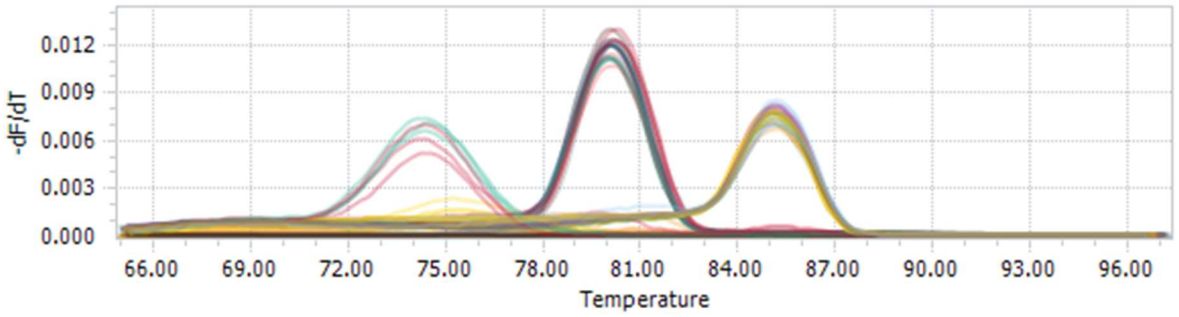

The decrease of fluorescence with time is shown as a function of temperature. Similarly, as in Fig 8, RT-PCR of the second donor for fibroblasts in the temperature range 71 °C to 78 °C showed primer dimers in the negative controls of RNA isolation and negative controls of RT-PCR (Figure 8). However, not all negative controls showed primer dimers. Furthermore, the courses of the melting curves are analogous to those shown in the first patient.

Figure 8. Melting curves for the RT-PCR of fibroblast samples of the second doner.

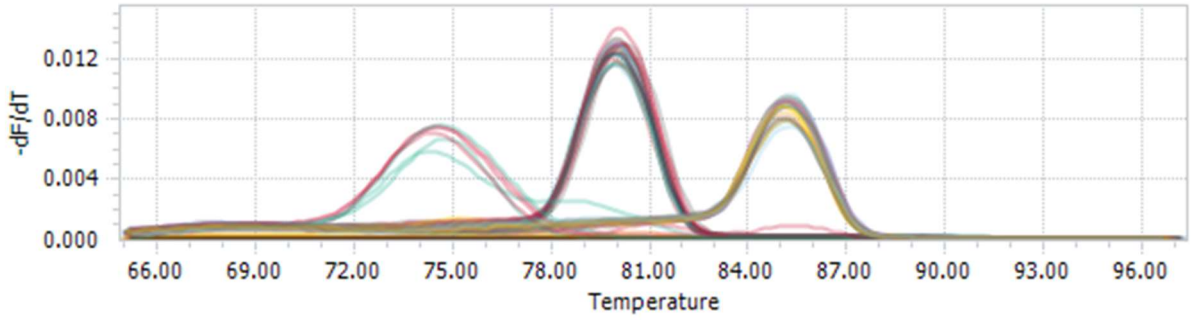

The decrease of fluorescence with time is shown as a function of temperature. Figure 9 shows the RT-PCR curves with osteoblast samples from the first patient. Again, primer dimers of the negative controls of RNA isolation and RT-PCR appeared in the same temperature range as in the previous measurements. The two further maxima at 80 °C for GAPDH and 86 °C for COL1A1 and COL5A1 exhibited the same decrease in fluorescence with time. The curves for the amplicons of the collagen primers COL1A1 and COL5A1 overlapped.

Figure 9. Melting curves for the RT-PCR of osteoblast samples of the first doner.

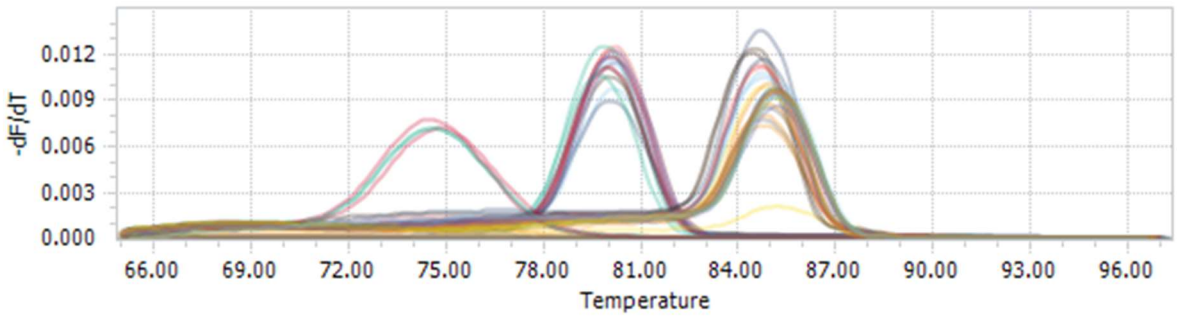

The decrease of fluorescence with time is shown as a function of temperature. After all previous measurements showed positive negative controls, the nuclease-free water was exchanged for fresh water for the negative controls of the second RT-PCR of osteoblasts.

As a result, melting curves revealed for the first time no third maxima in the original temperature range from 71 °C to 78 °C. It can therefore be assumed that the nuclease-free water used as a sample for the negative controls was contaminated (Figure 9). The negative control of the RNA isolation also exhibited no primer dimers and thus no contamination. It was also noticeable that the overlapping melting curves of the collagen primers COL1A1 and COL5A1 displayed varying degrees of decrease in fluorescence over time (Figure 10).

Figure 10. Melting curves for the RT-PCR of osteoblast samples of the second doner.

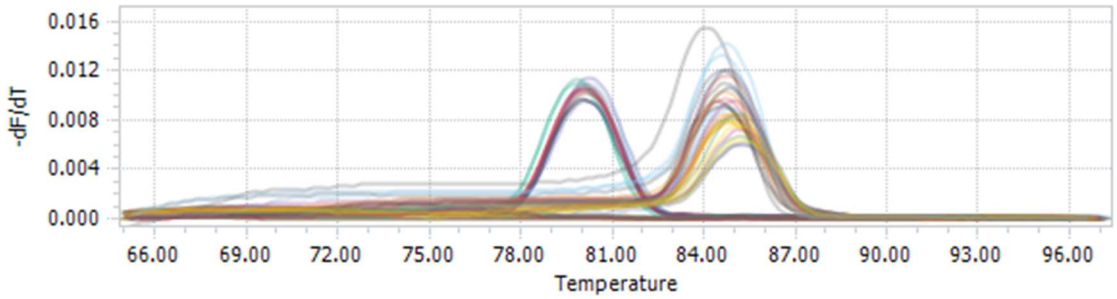

The decrease of fluorescence with time is shown as a function of temperature.

Semi-quantitative RT-PCR of fibroblasts

Figure 11 shows the mean Ct values for each eluate treatment for COL1A1, COL3A1 and GAPDH, respectively. All three primers used showed remarkably high Ct values in the range of 30 to 37 for at least one of the two negative controls. This is another indicator for the primer dimers. The Ct values of the control were found to be around 14 for COL1A1, COL3A1 and GAPPDH. The Ct values of the different treatments were lower than the control for both type I and III collagen. Only the treatment with Mem Lok® and algal membrane A2 showed slightly increased Ct values for GAPDH.

Figure 11 represents the type I and type III collagen expression of fibroblasts form patient one. Interestingly, all Argonaut™ and the algal membranes A3, A4 and A6 induced up-regulation of type I and type III collagen. The highest expression of type I collagen as well as type III was revealed after fibroblast treatment with Argonaut™ eluate. All measurements showed large errors in expression level calculation resulting from the slightly larger standard deviations of the GAPDH Ct values.

Figure 11. Semi-quantitative RT-PCR results of human fibroblasts from first patient.

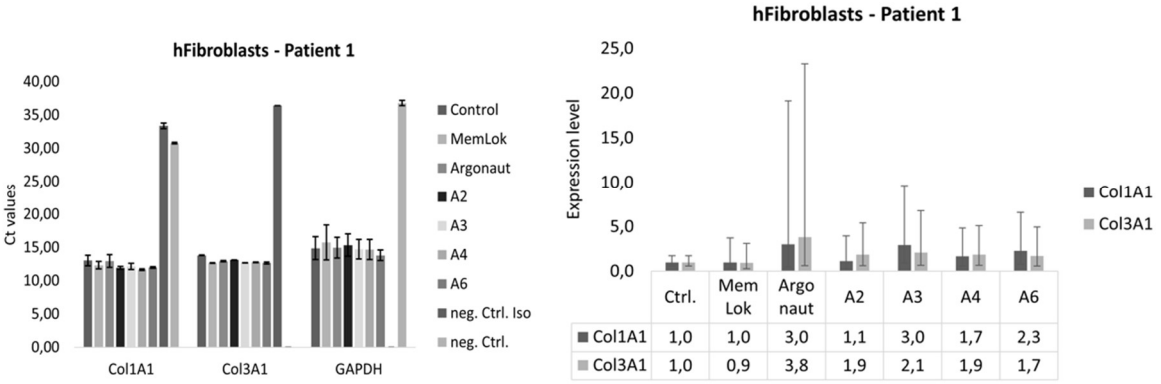

On the left side the mean Ct values are represented, on the right side the calculated expression levels of COL1A1 and COL3A1 of the different eluate treatments are shown. GAPDH was used as reference gene to determine the expression levels with the 2-ΔΔCt method.

In summary, the results of the fibroblasts of the first and second patient were not consistent. In addition, both measurements showed large errors, making a scientific evaluation of the results impossible.

Semi-quantitative RT-PCR of osteoblasts

Figure 12 show the results of osteoblast RT-PCR as well as the corresponding Ct values of the measurements. On the left part of Figure 12, it can be clearly seen that all Ct values of the different membranes are above those of the control. It can be clearly seen that all Ct values of the different membranes are above those of the control. Only the two negative controls of the COL1A1 samples showed increased Ct values of up to 30. Nothing was detected in the negative controls of the investigated genes COL5A1 and GAPDH. The diagram on the right side of Figure 12 represents the expression levels from both type I and type V collagen. Striking is that in all conditions COL1A1 was downregulated compared to the control. For both RM an expression level of only 50 % of the control was achieved. Algae membrane type A2 exhibited with 90 % the highest expression level but showed a large error. An upregulation of COL5A1 was exhibited by osteoblasts treated with the RMs and algae membrane type A6. Here as well, osteoblasts treated with RM Argonaut^{TM} showed with 2,5-fold expression the highest value. While type A2 with 90 % reached an expression level just below the control, the two remaining types A3 and A4 showed downregulated COL5A1 expression.

Figure 12. Semi-quantitative RT-PCR results of human osteoblasts from first patient.

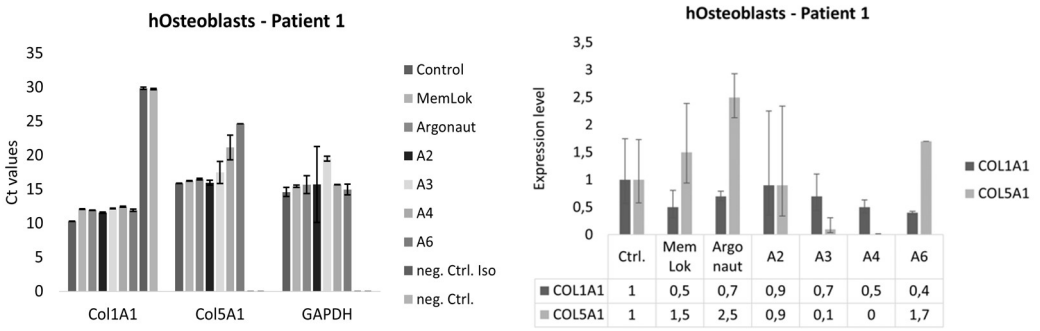

	Ctrl.	Mem Lok	Argo naut	A2	A3	A4	A6
COL1A1	1	0,5	0,7	0,9	0,7	0,5	0,4
COL5A1	1	1,5	2,5	0,9	0,1	0	1,7

On the left side the mean Ct values are represented, on the right side the calculated expression levels of COL1A1 and COL5A1 of the different eluate treatments are shown. GAPDH was used as reference gene to determine the expression levels with the 2-ΔΔCt method.

The Ct values for all measurements of the reference gene GAPDH were equally 13 with minimal deviations. Comparison of the two patients of osteoblast RT-PCR showed clear inconsistencies. Figure 13 in the second patient, the membrane treatments all led to a significant upregulation of COL1A1. Here, the RMs with an expression level of 300% for Mem-Lok® and 250% for Argonaut™ showed the most elevated levels. However, the algal membrane treatment also resulted in at least a 5-fold upregulation compared to the control. This does not correspond to the downregulation seen in the previous patient. The expression levels of COL5A1, on the other hand, showed an increase as in the first patient. Nevertheless, this is 10-fold higher in the osteoblasts of the second patient.

Figure 13. Semi-quantitative RT-PCR results of human osteoblasts from second patient.

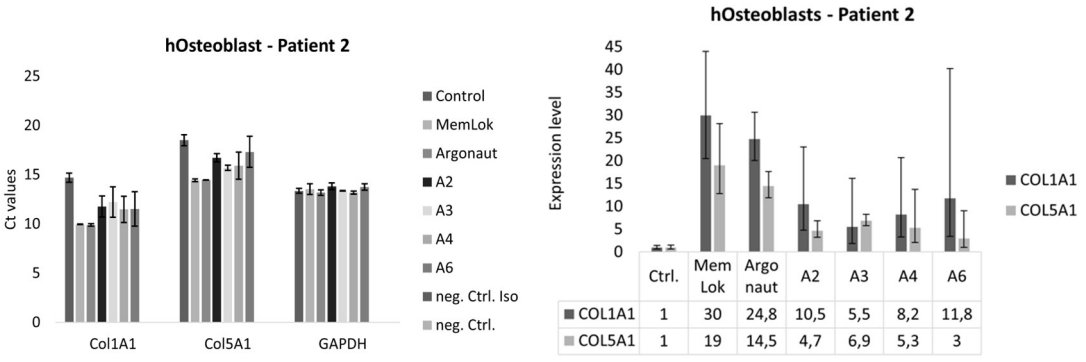

	Ctrl.	Mem Lok	Argo naut	A2	A3	A4	A6
COL1A1	1	30	24,8	10,5	5,5	8,2	11,8
COL5A1	1	19	14,5	4,7	6,9	5,3	3

On the left side the mean Ct values are represented, on the right side the calculated expression levels of COL1A1 and COL5A1 of the different eluate treatments are shown.

GAPDH was used as reference gene to determine the expression levels with the 2-ΔΔCt method.

Inactive positive control

The results of the osteoblastic proliferation on sandblasted-large grid-acid ached titanium surfaces (Dentcon® Dental Implant Systems, Ankara, Turkey) were not included in the quantitative/ comparative assessment. SEM results showed a high biocompatibility of the surface regarding the osteoblastic proliferation (Figure 14).

Figure 14. a) Sandblasted-large grid-acid ached titanium surface (Dentcon® Dental Implant Systems, Ankara, Turkey) by SEM prior to cell seeding. b) The proliferation characteristics and intercellular junctions showing the high biocompatibility of the surface.

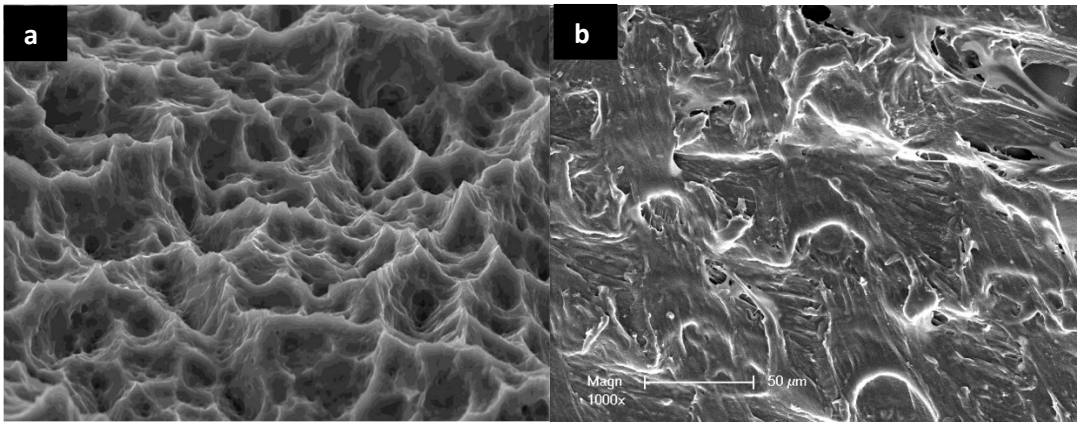

Discussion

The WST test showed that the cell viability and proliferation capacity of both cultured human fibroblasts and osteoblasts are at least equal to the control or even higher on the four algal membrane types A2 to A6. Especially the human osteoblasts revealed increased growth capacities on all four algal membranes, whereas the human fibroblasts exhibited equal values as the control. These results are consistent with the study of Sayin et al.[8] Surprisingly, osteoblasts on both RMs showed lower proliferation behavior than the control but also had larger errors of ± 0,167 for Mem-Lok® and ± 0,201 for Argonaut™. This indicates that either air bubbles during the measurement or pipetting error may falsified the results. Thus, the results

are unfortunately not consistent with the literature since both membranes underwent cytocompatibility assay before becoming commercially available. The osteoblasts showed the expected good proliferation behavior and cell viability on the RMs in the WST-1 assay.

Like the WST-1 assay, the MTT assay revealed that there was increased cell viability of human osteoblasts after treatment with the four algal membranes. For the RMs, they exhibited decreased proliferation compared to the control. This is consistent with the results of the WST-1 assay. Likewise, the growth capacity of fibroblasts on the reference membranes showed with high proliferation the same result as in the WST assay. Unfortunately, lower values were shown for the algal membranes than for the control, indicating a lower growth capacity of the cells. However, it is striking that there are comparatively large errors in the measurement of human fibroblasts. Moreover, since the study of Sayin et al. revealed cytocompatibility of algal membranes for fibroblasts, this measurement should be repeated.[8]

Lastly, the BrdU assays showed that the growth and proliferation capacity of cultured human fibroblasts and osteoblasts was at least equal or higher than that of all groups during the whole examination period. However, it was found in all three cytocompatibility assays that the osteoblasts were slightly more compatible with the algal membranes than the fibroblasts. The RMs showed a higher cytocompatibility for the fibroblasts.

In this work, WST-1, MTT and BrdU tests were used to evaluate and confirm the effects of different algal membranes on the cytocompatibility on humane fibroblasts and osteoblasts in vitro. In summary, all membranes showed similar results when compared to each other. Compared to the control group, the decreased proliferation rate of fibroblasts in the MTT test stood out. Since this is not in agreement with the literature, this measurement should be repeated. Nevertheless, it has been observed that all three assays showed similar tendencies. Especially the human osteoblasts revealed in all three assays a good proliferation behavior when treated with algal membranes. For a statistical evaluation and investigation of the significance of the results, all three assays should be repeated with at least cells from at least three additional patients.

The success of the PCR is already influenced by the design of the primers, so it is also crucial to optimize them.[16-18] All primers used were checked regarding their guanine and cytosine content, their melting temperature, amplicon length, etc. Particular attention was also paid to low 3'-selfcomplementarity to prevent primer dimerization.[17,18] However, improvements in guanine and cytosine base content could still be made. This is not in the optimal range of 50-

60 % for all primers, but for example 47,62 % for COL5A1 reverse and only 45 % for the reference gene primer GAPDH reverse.

Additionally, the choice of the reference gene must be discussed.[16,17] Although GAPDH is considered a robust housekeeping gene for RT-PCR expression assays and shows good expression in both human fibroblasts and human osteoblasts, reaction conditions may have an influence.[19,20] Thus, substances and leakages that diffused out of the algal membranes during eluate preparation could also have affected the expression of GAPDH. This needs to be further investigated.

The temperature gradient RT-PCR was performed to optimize the annealing temperature of the collagen primers and the reference gene primers.[20,21] An optimal binding temperature of 55,0 °C was determined. Due to the issue that the melting curve analysis indicated primer dimers presence, the temperature gradient PCR should be repeated but as a non-quantitative one. Instead, a PCR with following gel electrophoresis could be performed. During evaluation, the gels can then already be analyzed for primer dimers.[17,18] If any are present, for instance, the primer concentration can be adjusted.

As the melting curves revealed primer dimers in both negative controls of RNA isolation as well as RT-PCR the results of the RT-PCRs may be false positive and therefore cannot be evaluated.[12] Melt curve analysis verifies that a single specific product has been amplified.[16,17] When primer dimers are present, it can be assumed that they affect the fluorescence intensity and therefore an incorrect Ct value is generated.[11,12] Therefore, as mentioned in the previous chapter, the concentrations of the PCR components should be adjusted.[21] Since the EvoScript RNA SYBR Green I Master Kit already contains premixed master mix whose $Mg(OAc)_2$ concentration is optimized for SYBR® Green I applications, it is recommended to start adjusting the primer concentration. Further, the melting curve analysis is particularly effective when comparing results of template samples with data of not template controls.[17,18]

In addition to the NTC and negative control of RNA isolation, an internal positive control should be used, using a cell type that expresses the gene under investigation in all cases regardless of the reaction conditions.[11,12,20-22] For example, for COL1A1, RNA from HeLa cells could be used as a positive control, since they exhibit a high expression level of type I collagen (22). By using an internal positive control, proper performance of the PCR can be proven.[21,22]

Another control mechanism to achieve a higher level of precision among technical replicates is the passive reference dye ROX. It is an inert fluorescent dye that can be added to the

master mix of the RT-PCR. It is not affected by the amplification process, but is highly sensitive to e.g., air bubbles or condensation, which could lead to a change in overall fluorescence.[22,23]

Optimization should be performed at the level of semi-quantitative evaluation of RT-PCR using the ΔΔCt -method. For the ΔΔCt-method, the geometric efficiency is set to 2, which means that both the target and reference assays are 100 % efficient. Thus, it is fundamental to determine the efficiency of RT-PCR for each primer previously. To establish the PCR amplification efficiency, calibration curves for each quantified target should be measured.[11,12]

References

1.Prates LRC, Idiberto JZF, Ávaro JC. Main considerations on the use of biomembranes in implantology: A review. Dent Oral Craniofac Res 2017;4,1-5.

2.Retzepi M, Donos, N. Guided bone regeneration: biological principle and therapeutic applications. Clin Oral Implants Res 2010;21;567-76.

3.Wang PH, Huang BS, Horng HC, Yeh CC, et al. Wound healing. J Chin Med Assoc 2018;8194-101.

4.Sasaki JI, Abe GL, Li A, Thongthai P, et al. Barrier membranes for tissue regeneration in dentistry. Biomater Investig Dent 2021;8:54-63.

5.Elgali I, Omar O, Dahlin C, Thomsen P. Guided bone regeneration: materials and biological mechanisms revisited. Eur J Oral Sci 2017;125:315-37.

6.Hussain E, Wang LJ, Jiang B, Riaz S, et al. A review of the components of brown seaweeds as potential candidates in cancer therapy. RSC Advances 2016;6:12592-610.

7.Abd El-Hack ME, Abdelnour S, Alagawany M, Abdo M, et al. Microalgae in modern cancer therapy: Current knowledge. Biomed & Pharmacother 2019;111:42–50.

8.Sayin S, Kohlhaas T, Veziroglu S, Okudan E, et al. Marine Algae-PLA composites as de novo alternative to porcine derived collagen membranes. Mater Today Chem 2020;17:100276.

9.Präbst K, Engelhardt H, Ringgeler S, Hübner H. Basic colorimetric proliferation assays: MTT, WST, and Resazurin. Methods Mol Biol 2017;1601:1-17.

10.Crane AM, Bhattacharya SK. The use of bromodeoxyuridine incorporation assays to assess corneal stem cell proliferation. Methods Mol Biol 2013;1014:65-70.

11.Bustin SA, Benes V, Garson JA, Hellemans J, et al. The MIQE guidelines: minimum information for publication of quantitative real-time PCR experiments. Clin Chem 2009;55:611-22.

12.Perrotti V, Palmieri A, Pellati A, Degidi M, et al. Ricci L, Piattelli A, Carinci F. (2013). Effect of titanium surface topographies on human bone marrow stem cells differentiation in vitro. Odontology 2013;101:133-39.

13.Wang S, Zhong L, Li Y, Xiao D, et al. 2019). Up-regulation of PCOLCE by TWIST1 promotes metastasis in Osteosarcoma. Theranostics 2019;9:4342-353.

14.Liu J, Shen JX, Wu HT, Li XL, et al. Collagen 1A1 (COL1A1) promotes metastasis of breast cancer and is a potential therapeutic target. Discov Med 2018;25:211-23.

15.Radonić A, Thulke S, Mackay IM, Landt O, et al. Siegert W, Nitsche A. Guideline to reference gene selection for quantitative real-time PCR. Biochem Biophys Res Commun 2004;313:856-62.

16.Navarro E, Serrano-Heras G, Castaño MJ, Solera J. Real-time PCR detection chemistry. Clin Chim Acta 2015;439:231-50.

17.Rodríguez A, Rodríguez M, Córdoba JJ, Andrade MJ. Design of primers and probes for quantitative real-time PCR methods. Methods Mol Biol 2015;1275:31-56.

18.Thornton B, Basu C. Real-time PCR (qPCR) primer design using free online software. Biochem Mol Biol Educ 2011;39:145-54.

19.Lin J, Redies C. Histological evidence: housekeeping genes beta-actin and GAPDH are of limited value for normalization of gene expression. Dev Genes Evol 2012;222:369-76.

20.Zhao F, Maren NA, Kosentka PZ, Liao YY, et al. An optimized protocol for stepwise optimization of real-time RT-PCR analysis. Hortic Res 2021;8:179.

21.Bezold G, Krähn G, Peter RU. Falsch-negative Ergebnisse bei diagnostischer PCR wegen PCR-Inhibition: Überwachung mit internen Kontrollen. In: A. Plettenberg, W.N. Meigel, and I. Moll (Eds.), Dermatologie an der Schwelle zum neuen Jahrtausend. Springer Berlin Heidelberg: Berlin, Heidelberg, p. 49–52. 2000.

22.Liu S, Liao G, Li G. Regulatory effects of COL1A1 on apoptosis induced by radiation in cervical cancer cells. Cancer Cell Int 2017;17:73.

23.Wang G, Becker E, Mesa C. Optimization of 6-carboxy-X-rhodamine concentration for real-time polymerase chain reaction using molecular beacon chemistry. Can J Microbiol 2007;53:391-97.